INSTITUTE OF PHYSICS PUBLISHING JOURNAL OF PHYSICS B: ATOMIC, MOLECULAR AND OPTICAL PHYSICS

J. Phys. B: At. Mol. Opt. Phys. **38** (2005) 2187–2194 doi:10.1088/0953-4075/38/13/011

Application of x-ray nonlinear processes to the measurement of 10 fs to sub-ps of x-ray pulses

Kengo Moribayashi[1], **Takashi Kagawa**[2] **and Dong Eon Kim**[3]

[1] Japan Atomic Energy Research Institute, 8-1, Umemidai, Kizu-cho, Kyoto 619-0215, Japan
[2] Department of Physics, Nara Women's University, Nara 630-8506, Japan
[3] POSTECH, San 31, Hyoja-Dong, Namku, Pohang, Kyungbuk 790-784, Korea

E-mail: kengo@apr.jaeri.go.jp

Received 31 January 2005, in final form 28 April 2005
Published 14 June 2005
Online at stacks.iop.org/JPhysB/38/2187

Abstract

We study the measurement of pulses of short-pulse x-ray sources through multi-x-ray absorption processes, that is, x-ray nonlinear optical processes and the effect of the lifetime of the inner-shell excited states on the measurement theoretically. The x-ray pulses may be measured by an auto-correlation method, that is, by using double x-ray pulses and the x-ray emission from a multi-inner-shell excited state which has an intermediate state with a much shorter lifetime than the x-ray pulse. The necessary atomic data for the measurement are discussed and shown.

1. Introduction

The measurement of attosecond pulse x-rays has been reported [1–3] since the 21st century started and has attracted a great deal of attention. They have been measured by using electron wavepackets formed by ionization and controlled by strong laser fields. In addition, auto-correlation methods by using nonlinear x-ray processes have also been developed for the measurement of femtosecond x-ray pulses [4–7]. The nonlinear optical processes have developed the technology of high intensity lasers, such as the measurement of the amplitude, the phase, and so on, of lasers [4–8]. Therefore, x-ray nonlinear optical processes are also expected to be useful for high intensity x-ray (laser) sources [4–7, 9]. Recently, an x-ray pulse of 8 fs has been measured via the auto-correlation method by using double ionization of He by two-x-ray absorption [4].

Theoretical studies have predicted that high intensity lasers allow us high intensity short-pulse x-ray pulses with shorter wavelength, such as via Larmor radiation [10–12] or radiation damping [13]. These x-rays may have a lot of applications to the measurement of the ultrafast processes in material and biological sciences [14–16] and as excitation sources for inner-shell ionization lasers [17–21]. Moribayashi *et al* predicted that such high intensity, short wavelength x-rays may produce the multi-inner-shell excited state (MIES) or hollow atoms

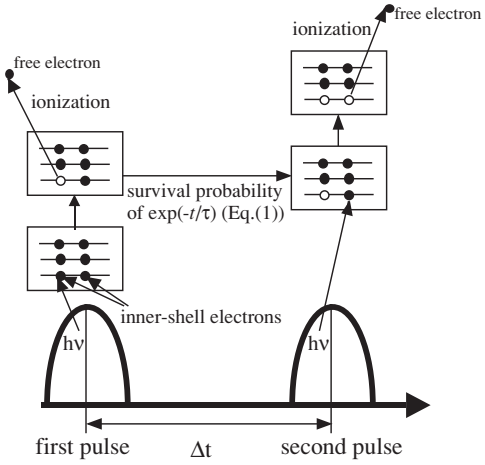

Figure 1. The production processes of MIES for $0 < t_X < \Delta t < \infty$.

(HA) as follows [17]. High intensity x-rays may produce an ultrafast inner-shell ionization processes. These processes may surpass any other atomic processes such as auto-ionization and radiation transition processes. As a result, multi-inner-shell ionizations predominate, leading to the formation of MIES or HA [17]. We take notice of the following point. Multi-inner-shell ionization processes are similar to the double ionization of He by two-photon absorption because of multi-x-ray absorption. Namely, for the measurement of a pulse of the short wavelength x-rays, multi-inner-shell ionization processes may be useful. In the case of the use of the double ionization of He, we should use the region of energy below the threshold of He^+ (about 54.4 eV) because of the infinite lifetime of He^+. The detailed reason will be discussed in section 2.

The aims of this paper are (i) to demonstrate that the multi-inner-shell ionization processes for the measurement of pulses from 10 fs to sub-picosecond and (ii) to list the necessary atomic data for the better selection of the target materials. We also study the contribution of the lifetimes of the inner-shell excited states (IES) to the measurement of pulses.

2. Simulation model

Here we treat the x-ray number (P_X) emitted from MIES and its application to the measurement of a short x-ray pulse by using an auto-correlation method. In this method, double x-ray pulses, which have time delay (Δt), are employed [4, 6]. The time delay is produced from the optical path difference [6].

For one x-ray pulse, $P_X = kI^2$ in the double-inner-shell ionization, where I and k are the intensity of x-rays and a constant of proportionality, respectively. For $\Delta t = \infty$, $P_X = 2kI^2$, while, in the case of $\Delta t = 0$, the x-ray intensity becomes $2I$, that is, $P_X = k(2I)^2$. Namely, P_X $(\Delta t = 0) = 2P_X$ $(\Delta t = \infty)$. For $0 < \Delta t < t_X$, P_X (Δt) becomes the value between P_X $(\Delta t = 0)$ and P_X $(\Delta t = \infty)$, where t_X is the pulse duration of x-rays. In the usual auto-correlation method, just when P_X $(\Delta t) = P_X$ $(\Delta t = \infty)$, Δt can be regarded as the pulse length. For $0 < t_X < \Delta t < \infty$, there is another process due to the production of MIES as shown in figure 1. The inner-shell excited states are produced from the first x-ray pulse and have a survival probability of

$$\exp(-t/\tau), \tag{1}$$

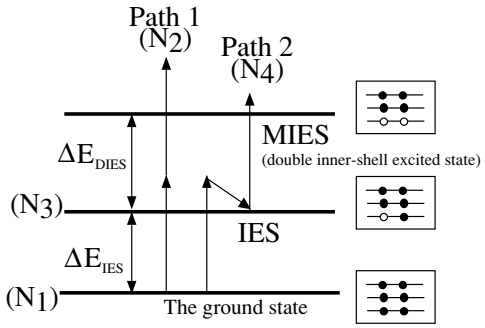

Figure 2. The paths of the production of MIES.

where τ is the lifetime of the inner-shell excited state. The survivor can be additionally ionized by a second x-ray pulse and as a result the MIES is produced. This process makes the measurement difficult. In the experiments of [4, 5], this process could not occur. Namely, they choose a smaller x-ray energy than the threshold of the ionization energy of He^+. Since the lifetime of He^+ is infinite, we should avoid this process in the double ionization of He by two-x-ray absorption. However, for MIES, we may be able to ignore this process by selecting a target material whose inner-shell excited state has a much shorter lifetime than the x-ray pulse. Then, we may also be able to treat x-ray energies larger than the threshold energy of inner-shell ionization from IES to MIES (ΔE_{DIES}). Further, this method may apply to not only coherent but also incoherent x-rays, which have a continuum energy distribution as seen in Larmor radiation [10–12].

Figure 2 shows the two paths for the production of the MIES. In the first path (path 1), two x-rays are absorbed within the decay time of $(He^+ + e^-)$. On the other hand, in the second path (path 2), IES is formed from the first x-ray absorption and the absorption of the second x-ray produces MIES from the IES. In the case of the double ionization of He by x-rays with an energy of 42 eV, the cross section of path 1 is about 10^{-52} cm^4 s [5]. This cross section is given in the perturbation approximation by

$$\sigma_{\mathrm{d}} \propto (h\nu)^2 \left| \sum_{\mathrm{k}'} \frac{\langle \mathrm{k}|r|\mathrm{k}'\rangle\langle \mathrm{k}'|r|0\rangle}{h\nu - E_{0\mathrm{k}'} + \mathrm{i}\Gamma_{\mathrm{k}'}} \right|^2, \tag{2}$$

where $h\nu$, $E_{0\mathrm{k}'}$ and $\Gamma_{\mathrm{k}'}$ are the energy of x-rays, the sum of the threshold energy of He and the energy of the photo-ionized electron (in this case, $h\nu = E_{0\mathrm{k}}$) and the existence time of the ionized electron in He, respectively, and the states $|0\rangle$, $|\mathrm{k}\rangle$ and $|\mathrm{k}'\rangle$ represent those for He, $(He^+ + e^-)$ and $(He^{2+} + 2e^-)$, respectively. Roughly speaking, since the single-ionization cross section is $\sigma_s \propto (h\nu)[\langle \mathrm{k}'|r|0\rangle]^2 \propto (h\nu)^{-3}$ [22], σ_{d} becomes smaller according to $(h\nu)^{-6}$. At the x-ray energy of 60 eV, where the one-photon ionization occurs from the He^+ ion, $\sigma_{\mathrm{d}} \sim 10^{-53}$ cm^4 s. On the other hand, the single-ionization cross sections from He (σ_{s1}) and He^+ (σ_{s2}) are derived to be $\sigma_{\mathrm{s1}} \sim \sigma_{\mathrm{s2}} \sim 10^{-18}$ cm^2 from the calculation by Cowan's code [23]. In order to compare the populations of He^{2+} produced through path 1 and path 2, we solve the following rate equations,

$$\dot{N}_2 = R_{12}N_1, \qquad \dot{N}_3 = R_{13}N_1, \qquad \dot{N}_4 = R_{34}N_3, \tag{3}$$

where N_1, N_2, N_3 and N_4 are the populations of the ground state of He, He^{2+} through path 1, He^+ and the He^{2+} through path 2, respectively (shown in figure 2) and R_{ab} (σ_{ab}) is the rate (cross

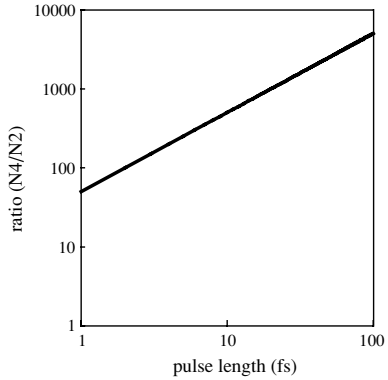

Figure 3. The pulse length of x-rays versus ratio (N_4/N_2) for the double ionization of He by two-x-ray absorption and an x-ray energy of 60 eV.

section) for the ionization process from the a state to the b state. The relationship between R_{ab} and σ_{ab} is given by

$$R_{12} = \frac{I^2\sigma_d}{(h\nu)^2}, \qquad R_{13(34)} = \frac{I\sigma_{13(34)}}{h\nu}, \tag{4}$$

where I is the intensity of x-rays. Figure 3 shows the ratio of N_4 with N_2 (N_4/N_2) as a function of pulses of x-rays for $I = 10^{12}$ W cm^{-2}. We should note that the ratio is independent of the x-ray intensities (not shown here). The ratio becomes larger according to the x-ray pulse length. Even with an x-ray pulse of 1 fs, the ratio is more than 50. Therefore, in the case of an x-ray energy of 60 eV, path 2 dominates for the production of He^{2+}. We can guess that this comes from the interaction time of the intermediate state ($He^+ + e^-$ for path 1, He^+ for path 2) with x-rays, which corresponds to $\Gamma_{k'}$ and the x-ray pulse for path 1 and path 2, respectively. We should note that the interaction time corresponds to the smaller value between the x-ray pulse and the lifetime of IES in the production process of MIES. In this paper, we treat the lifetime of IES of more than 1 fs and an x-ray pulse of more than 10 fs, which are much longer than $\Gamma_{k'}$. Therefore, we consider only path 2.

The method of calculation of the number of x-rays emitted from MIES employed here is the same as that in [24].

3. Results and discussions

Figures 4(a) and (b) show r defined by the following equation as a function of Δt for the x-ray emissions from MIES and HA of Si produced by double-pulse x-rays of 20 fs and 200 fs, respectively:

$$r = \frac{(P_N(\Delta t) - P_N(\infty))}{(P_N(0) - P_N(\infty))}, \tag{5}$$

where $P_N(\Delta t)$ is the x-ray number from MIES or HA for Δt. We should note that r is defined as $r = 1$, for $\Delta t = 0$, and $r = 0$, for $\Delta t = \infty$. The atomic processes treated here are the same as those in figure 1 in [24]. The corresponding n values for the lines shown in figure 3 represent the number of 2p states of MIES or HA. For example, the n values of 0, 2 and 5 correspond to the states of $1s^22s^23s^2$, $1s^22s^22p^23s^2$ and $1s^22s^22p^53s^2$, respectively. We have also found that the r values are independent of the intensities and energies of the x-rays

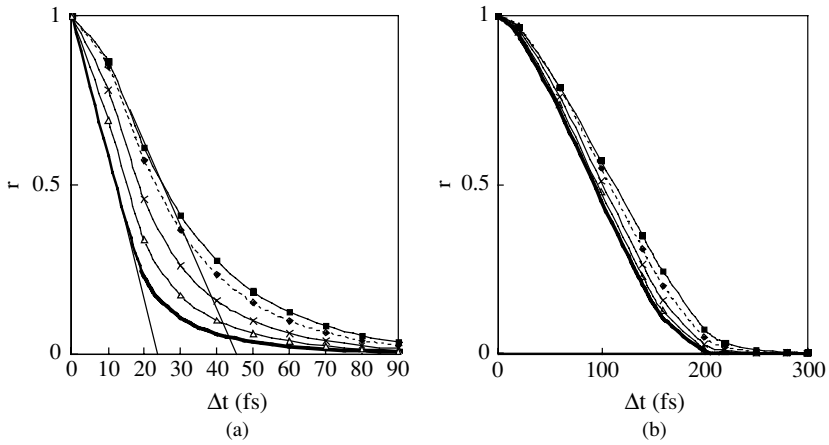

Figure 4. r (defined in equation (4)) versus time delay (Δt) for the x-ray emission from MIES of Si. The n values correspond to the number of the 2p states: x-ray pulses are (a) 20 fs and (b) 200 fs. The lines with symbols —, –Δ–, –×–, –●– and –■– correspond to the n values of 0, 1, 2, 3 and 4, respectively.

(not shown here), though it is the case where the energies are larger than the threshold of MIES. The decay of population of IES is controlled by equation (1). As time goes on, the population decays more slowly. The shape for equation (1) appears in figure 4(a) and causes a large error for the measurement of the pulse. Therefore, the pulse should be derived from the crossing point between the target line (shown in figure 4(a) for $n = 0$ and 4 as solid lines) and $r = 0$. For the x-ray pulse of 20 fs (figure 4(a)), it is seen that the pulses estimated here become more accurate as n decreases. On the other hand, for the 200 fs x-ray pulse (figure 4(b)), the x-ray pulse may be measured within an error of 10% for all n. We have guessed that this is caused by the lifetime of the intermediate states (the $(n + 1)$ state) as shown in figure 1. The lifetime of the IES, MIES and HA can be estimated from table 1 in [1]. For example, those of IES and HA are about 25 and 5 fs, respectively.

From here, in order to make the analysis simple, we treat only the double-inner-shell excited states (DIES) ($n = 4$) for MIES. We study the effect of the lifetime on r. Figures 5(a) and (b) are the same as figure 4 for the lifetime of 1 and 10 fs, respectively. We treat x-ray pulses of 20, 50 and 80 fs. We can measure more accurately the x-ray pulses for the lifetime of 1 fs than that of 10 fs. In the case of the lifetime of 10 fs, the crossing points between the target line and $r = 0$ are located at $\Delta t \sim 28$, 54 and 81 fs for the x-ray pulses of 20, 50 and 80 fs, respectively. Figure 6 shows the error caused due to the lifetime as a function of x-ray pulse duration for a lifetime of 10 fs. From this figure, we have concluded that a lifetime about six times smaller than the x-ray pulse duration is required to achieve an error of 5%. Figure 7 is the same as figure 5 for various lifetimes of IES. We have found that we may be able to measure a more accurate pulse length as the lifetime becomes shorter. Namely, when we measure the x-ray pulse from the x-ray emission from DIES, we must consider the lifetime of the IES and we need to use a target with much shorter lifetimes of IES. However, a target with a longer lifetime can produce DIES easier as seen in figure 3. Therefore, we should select a better target carefully from the atomic data.

The necessary atomic data for this measurement are mainly the threshold energies of inner-shell (ΔE_{IES}) and double-inner-shell ionization (ΔE_{DIES}) and the lifetime of IES, where ΔE_{IES} and ΔE_{DIES} are shown in figure 2. Table 1 lists the values of ΔE_{IES} and ΔE_{DIES}

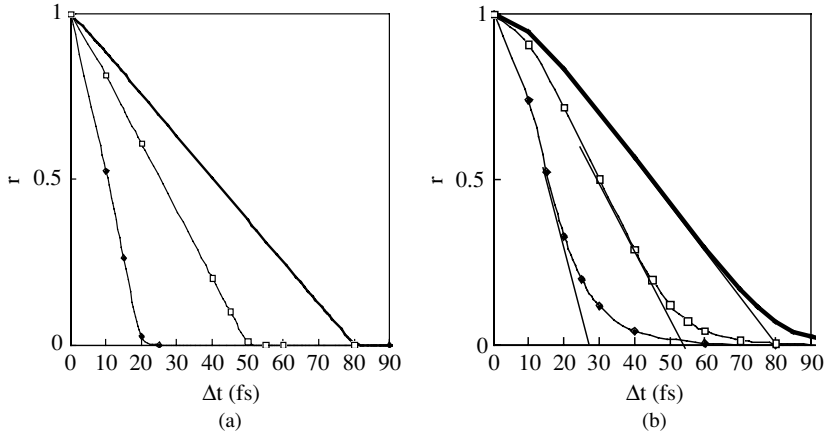

Figure 5. The same as figure 4 for $n = 4$, various x-ray pulse lengths, the lifetime of IES of (a) 1 fs and (b) 10 fs. The lines with symbols –●–, –□– and — correspond to the x-ray pulse lengths of 20 fs, 50 fs and 80 fs, respectively.

Table 1. The threshold energy from the ground state to IES (ΔE_{IES}) and from IES to DIES (ΔE_{DIES}) for (a) 1s and (b) 2p electrons versus atomic number: ΔE_{IES} and ΔE_{DIES} are defined in figure 2.

Atomic number	ΔE_{IES} (eV)	ΔE_{DIES} (eV)	Atomic number	ΔE_{IES} (eV)	ΔE_{DIES} (eV)
	(a)			(b)	
3	64	108	11	37	61
4	123	180	12	56	83
5	201	269	13	81	110
6	297	376	14	108	140
7	412	502	15	139	174
8	545	646	16	172	210
9	697	810	17	209	249
10	868	992	18	249	292
11	1077	1215	19	301	348
12	1309	1462	20	358	409
13	1565	1733	21	412	464
14	1833	2032	22	469	522
15	2154	2351	23	528	584
16	2482	2694	24	584	639
17	2834	3060	25	657	716
18	3209	3450	26	727	788
			27	799	862
			28	875	940
			29	946	1010
			30	1037	1105
			31	1135	1207
			32	1238	1314
			33	1345	1426
			34	1458	1543
			35	1576	1664
			36	1698	1791

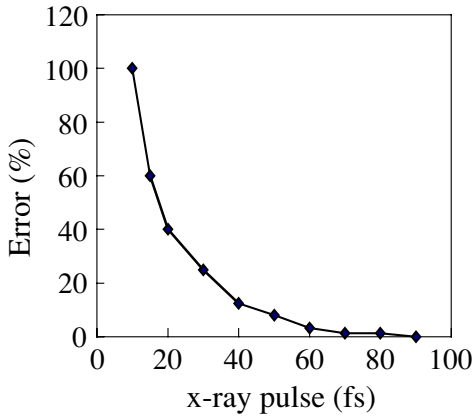

Figure 6. The error (%) caused due to the lifetime versus x-ray pulses for the lifetime of 10 fs.

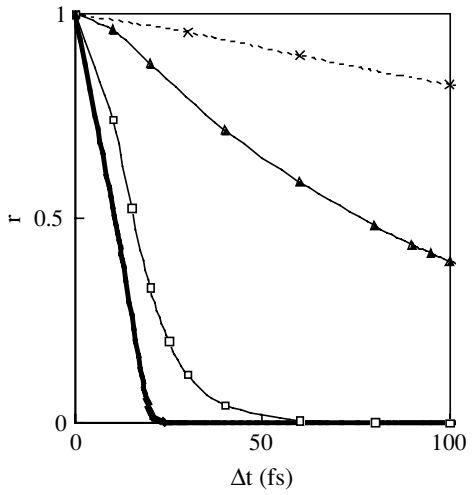

Figure 7. The same as figure 4 for an x-ray pulse of 20 fs and various lifetimes. The lines with symbols —, –□–, –▲–, and –×– correspond to the lifetimes of 1 fs, 10 fs, 100 fs and 500 fs, respectively.

calculated by Cowan's code [23] for the 1s and 2p electrons of various atoms. The lifetimes of the IES have been shown in [25]. Since the ionization cross sections show the maximum value near the threshold [26], we should choose target materials according to the energy of our x-ray pulses.

4. Conclusions

We have proposed the measurement of pulses of short-pulse x-ray sources by using multi-inner-shell ionization processes produced by double x-ray pulses. We have found that the lifetimes of the inner-shell excited state and multi-inner-shell excited states give a significant contribution to the measurement of the pulse length. We have recommended that the lifetime should be about six times smaller than the x-ray pulse. The suitable target materials may be decided from atomic data shown here and in [25, 26].

Acknowledgments

We wish to thank Professors T Tajima and K Namikawa and Drs M Mori, J Koga, H Daido, M Yamagiwa, A Nagashima and T Kimura for their useful discussions and the core university program between KOSEF and JSPS for support. D E Kim would like to thank the Korea Research Foundation (KRF-2000-015-DP0175) for support. D E Kim would also like to thank the Korean Science and Engineering Foundation for support through the National Research Laboratory Project.

References

[1] Itatani J, Niikura H and Corkum P B 2004 *Phys. Scr.* T **110** 112
[2] Hentschel M *et al* 2001 *Nature* **414** 509
[3] Niikura H *et al* 2002 *Nature* **417** 917
[4] Nabekawa Y, Hasegawa H, Takahashi E J and Midorikawa K 2005 *Phys. Rev. Lett.* **94** 043001
[5] Hasegawa H, Takahashi E J, Nabekawa Y, Ishikawa K L and Midorikawa K 2005 *Phys. Rev.* A **71** 023407
[6] Sekikawa T, Katsura T, Miura S and Watanabe S 2002 *Phys. Rev. Lett.* **88** 193902
[7] Ishikawa K and Midorikawa K 2002 *Phys. Rev.* A **65** 043405
[8] Iaconis C and Walmsley I A 1998 *Opt. Lett.* **23** 792
[9] Novikov S A and Hopersky A N 2000 *J. Phys. B: At. Mol. Opt. Phys.* **33** 2287
[10] Ueshima Y, Kishimoto Y, Sasaki A and Tajima T 1999 *Laser Part. Beams* **17** 45
[11] Lee K, Cha Y H, Shin M S, Kim B H and Kim D 2003 *Phys. Rev.* E **67** 026502
[12] Lee K, Cha Y H, Shin M S, Kim B H and Kim D 2003 *Opt. Exp.* **11** 309
[13] Zhidkov A, Koga J, Sasaki A and Uesaka M 2002 *Phys. Rev. Lett.* **88** 185002
[14] Guo T, Petruck C R, Jimenez R, Ràksi F, Squier J, Walker B, Wilson K R and Barty C P J 1997 *Proc. SPIE* **3157** 84
[15] Kandori H, Sasabe H, Nakanishi K, Yoshizawa T, Mizukami T and Shichida Y 1996 *J. Am. Chem. Soc.* **118** 320
[16] Akimoto S, Takaichi S, Ogata T, Nishimura Y, Yamazaki I and Mimuro M 1996 *Chem. Phys. Lett.* **260** 147
[17] Moribayashi K, Sasaki A and Tajima T 1998 *Phys. Rev.* A **58** 2007
[18] Moribayashi K, Sasaki A and Tajima T 1999 *Phys. Rev.* A **59** 2732
[19] Kapteyn H C 1992 *Appl. Opt.* **31** 4391
[20] Moon S J, Eder D C and Strobel G L 1994 *AIP Conf. Proc.* **332** 262
[21] Kim D, Son S H, Kim J H, Toth C and Barty C P J 2001 *Phys. Rev.* A **63** 023806
[22] Zel'dovich Y B and Raizer Y P 1966 *Physics of Shock Waves and High Temperature Hidrodynamics Phenomena* (New York: Academic) pp 265
[23] Cowan R D 1968 *J. Opt. Soc. Am.* **58** 808
[24] Moribayashi K, Kagawa T and Kim D E 2004 *J. Phys. B: At. Mol. Opt. Phys.* **37** 4119
[25] Rahkonen O K and Krause M O 1974 *At. Data Nucl. Data Tables* **14** 139
[26] Yen J J and Lindau I 1985 *At. Data Nucl. Data Tables* **32** 1